

Identifying Unmeasured Confounders in Panel Causal Models: A Two-Stage LM-Wald Approach

Bang Quan Zheng

University of Texas at Austin

2025

Abstract

Panel data are widely used in political science to draw causal inferences. However, these models often rely on the strong and untested assumption of sequential ignorability—that no unmeasured variables influence both the independent and outcome variables across time. Grounded in psychometric literature on latent variable modeling, this paper introduces the Two-Stage LM-Wald (2SLW) approach, a diagnostic tool that extends the Lagrange Multiplier (LM) and Wald tests to detect violations of this assumption in panel causal models. Using Monte Carlo simulations within the Random Intercept Cross-Lagged Panel Model (RI-CLPM), which separates within- and between-person effects, I demonstrate the 2SLW’s ability to detect unmeasured confounding across three key scenarios: biased correlations, distorted direct effects, and altered mediation pathways. I also illustrate the approach with an empirical application to real-world panel data. By providing a practical and theoretically grounded diagnostic, the 2SLW approach enhances the robustness of causal inferences in the presence of potential time-varying confounders. Moreover, it can be readily implemented using the R package lavaan.

[Word count: 6,000]

Keywords: Panel data analysis, sensitivity analysis, RI-CLPM, measurement

1 Introduction

In recent decades, political scientists have increasingly focused on the methodological challenges of identifying causal mechanisms, often turning to longitudinal panel data analyzed through approaches such as cross-lagged panel models (CLPMs), latent growth curve models, and random intercept cross-lagged panel models (RI-CLPMs). In line with this trend, researchers have adopted structural equation modeling (SEM) with latent variables to measure unobserved constructs and uncover underlying causal pathways—particularly when experimental designs are impractical (Chiu et al., 2025). For example, scholars have examined causal relationships using panel data such as those between partisanship and core values (Goren, 2005) and between authoritarianism and Republican support (Luttig, 2021), personality and political preferences (Bakker, Schumacher, & Rooduijn, 2021), the ideological roots of moral intuition (Hatemi et al., 2019), and the effects of political trust on social trust over time (Dinesen et al., 2022). These examples reflect a broader wave of research that uses panel data to uncover the dynamics of political attitudes and behavior. Unmeasured confounding in panel models poses a persistent challenge, however, with significant implications for both theoretical understanding and policy formulation. Current methods often fail to adequately address this issue.

While panel analyses offer valuable leverage for identifying causal relationships, they rely on a critical assumption: sequential ignorability—the idea that no unmeasured factors influence both the independent and outcome variables across waves. When this assumption is violated, unmeasured confounding can introduce spurious associations, distorting causal estimates and masking true underlying mechanisms. Sensitivity analysis is essential for assessing how unmeasured confounding may bias results (Acharya et al., 2016; Blackwell, 2014; Imai et al., 2010; Imai et al., 2011; Imai et al., 2013), but existing methods are limited for panel models with multiple waves and complex interdependencies. They typically examine one independent variable at a time and often fail to account for latent residual correlations or unmeasured confounders that may influence multiple pathways

simultaneously (Harring et al., 2017). Manual variable selection in sensitivity analysis introduces subjectivity, reducing reliability and limiting the detection of confounders (Blackwell, 2014).

Moreover, prior research shows that complex models—with more parameters, limited sample sizes, and intricate temporal structures—are especially prone to specification errors, including overlooked confounders (Zheng & Bentler, 2025). This issue is particularly acute in multi-wave panel models that include autoregressive (AR) and cross-lagged (CL) effects, where stable individual differences, if uncontrolled, can bias estimates of within-person dynamics (Feldman et al., 2025). As scholars have noted, analytic models in this area often overestimate causal effects (Bakker, Schumacher, & Rooduijn, 2021; Lucas, 2023). Such biases can carry significant theoretical and policy implications.

To address these challenges, this study builds on the 'improved LM test' proposed by Zheng and Bentler (2025) and introduces a two-stage sequential approach that combines the strengths of the Lagrange Multiplier (LM) test and the Wald test to detect potential confounders in panel causal models. I term this the Two-Stage LM-Wald (2SLW) approach—a data-driven method for detecting both observed and unobserved confounders, identifying path misspecifications and unmeasured confounders in SEM-based panel models, and evaluating the influence of latent and observed variables while accounting for measurement error. Drawing on psychometric literature, the proposed approach first applies the LM test to identify potential unmeasured confounders and subsequently uses the Wald test to pinpoint which specific cross-lagged or autoregressive paths are affected. The 2SLW method is applicable to both continuous and discrete variables and is designed for parametric models.

I demonstrate the 2SLW approach using RI-CLPMs, which preserve the core dynamics of CLPMs while separating stable between-person differences from within-person changes, providing a more general framework for specification diagnostics. Monte Carlo simulations show that 2SLW effectively detects unmeasured confounders in three common situations: when a hidden factor biases the

relationship between the independent and outcome variables, distorts a mediation pathway, or alters a direct effect. I also apply the method to real panel data with discrete variables measured across three waves, further illustrating its practical usefulness. While this paper focuses on demonstrating 2SLW within the RI-CLPM, the method is also applicable to other longitudinal panel models, such as second-order RI-CLPM and standard CLPM (see the Appendix). Importantly, the 2SLW procedure can be readily implemented using the widely used R package ‘*lavaan*,’ making it accessible to applied researchers.

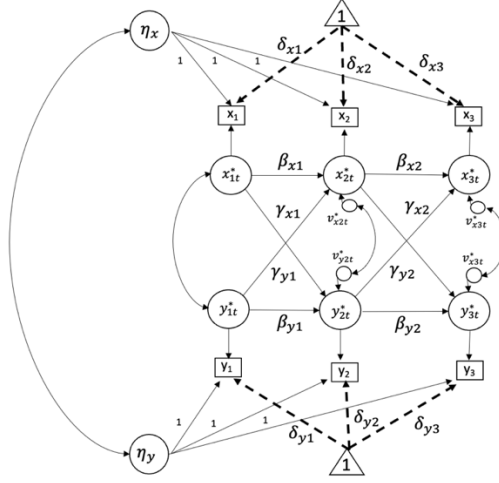
This paper proceeds as follows: Section 2 reviews the RI-CLPM in panel causal inference. Section 3 discusses challenges in conventional sensitivity analysis for panel models. Section 4 reviews the LM and Wald tests. Section 5 introduces the simulation setup, followed by simulation results in Section 6. Section 7 presents an empirical illustration. Finally, Section 8 offers discussion and conclusions.

2 RI-CLPM as a Framework for Panel Causal Inference

The RI-CLPM has become a widely used method for analyzing causal relationships in longitudinal data in the social and behavioral sciences. It extends the traditional CLPM framework by addressing a key limitation: the conflation of between-person differences with within-person changes. By separating stable between-person differences from within-person dynamics, the RI-CLPM helps correct for bias introduced by time-invariant confounders—a core weakness of standard CLPMs (Hamaker et al., 2015; Usami et al., 2019). This distinction helps correct for bias that arises when time-invariant confounders are ignored—a major limitation of standard CLPMs (Lucas, 2023). The CLPM assumes that all relevant stable traits are either measured or irrelevant. When this assumption is violated, unobserved stable factors can confound the cross-lagged estimates. Although the RI-CLPM captures stable between-person variance through random intercepts, it is still vulnerable to time-varying unmeasured confounders. Additionally, in standard CLPMs, unaccounted measurement error

can distort AR and CL estimates, leading to misleading conclusions about within-person stability and change (Feldman et al., 2025; Hamaker et al., 2015; Lucas, 2023; Mund et al., 2021).

Figure 1. Diagram of RI-CLPM



As Figure 1 illustrates, RI-CLPMs help identify the causal direction and strength of relationships by examining how one variable at an earlier time point predicts another at a later time point in multi-wave panel data, while controlling for prior levels of both variables. For statistical illustration, I consider a simple bivariate model. Suppose we are interested in examining the temporal reciprocal relationships between two random variables, x_i and y_i . Also, I use x_{it} and y_{it} to denote the measurements at time point t for individual i ($i = 1, \dots, n; t = 1, \dots, T$). The RI-CLPM can be expressed as follows:

$$x_{it} = \delta_{xt} + \eta_{xi} + x_{it}^*, \quad (1)$$

$$y_{it} = \delta_{yt} + \eta_{yi} + y_{it}^*. \quad (2)$$

Here let δ_{xt} and δ_{yt} represent temporal group means at time point t , and η_{xi} and η_{yi} are individual-level time-invariant trait factors. In the RI-CLPM δ_{xt} and δ_{yt} aim to capture mean growth trajectories and x_{it}^* and y_{it}^* are temporal deviation terms, which capture the temporal within-person

deviations from the means of each person, i . As such, we need to partition the between-person level and within-person level to understand the dynamics between the effect of time-invariant stable trait factors and time-varying occasion-specific factors. In the context of equations 1 and 2, x_{it}^* and y_{it}^* capture the temporal deviations from the expected values of x_{it} and y_{it} , that is, $\delta_{xt} + \eta_{xi}$ and $\delta_{yt} + \eta_{yi}$. Thus, the within-person reciprocal relations are modeled using lagged effects and temporal trait factors (Hamaker et al., 2015; Usami, 2021). The within-person reciprocal relations are defined as:

$$x_{it}^* = \beta_x x_{i(t-1)}^* + \gamma_x y_{i(t-1)}^* + v_{xit}, \quad (3)$$

$$y_{it}^* = \beta_y y_{i(t-1)}^* + \gamma_y x_{i(t-1)}^* + v_{yit}, \quad (4)$$

where β_x and β_y are AR parameters that measure the within-person stability of x and y , respectively. Notably, β_x and β_y do not necessarily reflect the stability of individuals' rank order across occasions; rather, they capture the magnitude of the within-person carry-over effect. γ_x and γ_y are CL parameters that capture reciprocal relations between x and y . v_{xit} and v_{yit} are the residuals, which are assumed to follow a normal distribution with an unknown variance $N(0, \sigma^2)$.

$$\begin{bmatrix} x_{it} \\ y_{it} \end{bmatrix} = \begin{bmatrix} \delta_{xt} \\ \delta_{yt} \end{bmatrix} + \begin{bmatrix} \eta_{xi} \\ \eta_{yi} \end{bmatrix} + \begin{bmatrix} \beta_x & \gamma_x \\ \beta_y & \gamma_y \end{bmatrix} \begin{bmatrix} x_{i(t-1)}^* \\ y_{i(t-1)}^* \end{bmatrix} + \begin{bmatrix} v_{xit} \\ v_{yit} \end{bmatrix} \quad (5)$$

It is important to note that β_x and β_y do not necessarily represent the stability of the rank order of individuals from one occasion to another; instead, they indicate the magnitude of within-person carry-over effect (Hamaker et al., 2015). However, their residuals may share common variance, which can be expressed as:

$$\rho = \text{Cor}[v_{xit}, v_{yit}], \quad (6)$$

where ρ denotes the correlation between v_{xit} and v_{yit} . The sequential ignorability assumption implies $\rho = 0$; if $\rho \neq 0$ it indicates the presence of unmeasured confounder affecting both the independent and outcome variables.

Although RI-CLPM addresses stable, trait-level confounders, it cannot account for unobserved confounders that vary over time or for concurrent effects, both of which can bias within-person estimates. Incorporating observed time-varying confounders and examining concurrent structures can improve validity. When an unmeasured latent variable influences both independent and outcome variables—or multiple variables within a cross-lagged structure—it violates sequential ignorability and can bias results through shared variance (Lucas, 2023). Misattributing shared variance to specified paths rather than omitted confounders can bias coefficients—potentially inflating, weakening, or reversing their sign—so that even small unaccounted influences may distort causal interpretation.

2.2 Key Differences between CFA and RI-CLPM

This study adapts the joint LM and Wald tests—originally developed by Zheng and Bentler (2025) for use in Confirmatory Factor Analysis (CFA)—to the context of panel causal models, where their application presents important methodological distinctions. While the statistical foundations of these tests remain consistent, several key differences between CFA and RI-CLPMs warrant careful attention. First, CFA assumes a stationary structure with stable loadings and residuals, whereas RI-CLPM models dynamic processes over time. RI-CLPM introduces random intercepts and time-ordered constraints, increasing complexity and limiting the flexibility of the covariance structure. Consequently, LM test statistics in RI-CLPMs may appear inflated or misleading due to misspecification or convergence issues. Second, LM tests in CFA typically identify local misfit (e.g., residual correlations) under the assumption of local independence. In contrast, RI-CLPM’s temporal interdependence and feedback loops complicate such diagnostics. LM tests in this context often fail to detect dynamic interactions or suppressor effects, leading to potentially misleading modification suggestions. Third, panel model misfit is often global—driven by violations of stationarity, measurement invariance, or residual autocorrelation—which LM tests may not capture. The random intercepts in RI-CLPM absorb

between-person variance, potentially masking within-person misspecifications. Additionally, measurement error can further reduce the test's power, causing false negatives or prompting overfitting by suggesting paths that conflict with theory (Zheng & Valente, 2023).

In sum, although the LM test framework can be extended to RI-CLPMs, its application is far from straightforward. The dynamic, multilevel nature of panel models requires careful interpretation of results and underscores the need for diagnostic tools specifically designed for longitudinal causal inference. Given their sensitivity to model structure, misspecification, and latent confounding, more robust, tailored diagnostics are essential.

3 Existing Challenges to Sensitivity Analysis & Research Strategy

Sensitivity analysis plays a crucial role in evaluating the robustness of causal conclusions, particularly in the presence of potential unmeasured confounders. While political methodologists have developed formal tools for sensitivity analysis (Acharya et al., 2016; Blackwell, 2014; Imai et al., 2010; Imai et al., 2011), these methods do not readily extend to complex longitudinal models such as the RI-CLPM or other panel causal models. In these settings, confounding is more nuanced: time-invariant and time-varying unobserved factors may influence multiple variables across waves, introducing bias even when initial exposures are randomized.

However, in panel models like the RI-CLPM—which include reciprocal relationships, repeated measurements, and latent constructs—the potential for unmeasured confounding is both more complex and harder to detect. Time-invariant confounders open multiple backdoor paths, introducing bias into the estimated causal effects (Imai et al., 2016). That is, confounders may simultaneously affect multiple variables across time, not just the residuals of mediator and outcome. Moreover, traditional sensitivity analyses designed for static models are not well-suited to detect the broader model misfit that arises when these confounding structures are present.

A persistent challenge in panel causal analysis with intermediate or time-varying variables is that, even when the initial exposure is randomized, subsequent variables—such as mediators, attitudes, or behaviors—may still be endogenous. These variables may be influenced by stable traits, prior experiences, or other latent factors, which also affect downstream outcomes. For example, in studies of immigration attitudes, both media exposure and policy preferences may be shaped by underlying ideological dispositions or ethnocentric orientations that are rarely measured directly. As a result, estimates of causal effects may conflate genuine relationships with spurious associations caused by unmeasured confounders or self-selection processes. This issue is particularly acute in dynamic models where feedback loops and reciprocal causation are possible (Bullock et al., 2010; Holland, 1988; Imai et al., 2011; MacKinnon, 2008; MacKinnon & Pirlott, 2015; Pearl, 2001; Robins & Greenland, 1992). To address these challenges, researchers need diagnostic tools capable of assessing model specification and detecting unaccounted confounding pathways—particularly in longitudinal SEMs. The 2SLW approach introduced in this paper offers a novel method for identifying unmeasured confounding in RI-CLPMs and model specification search.

3.1 Research Strategy

The illustration of the 2SLW method proceeds in three steps. First, I generate data from a population RI-CLPM that includes omitted latent confounders, then fit an analysis model that excludes them—mimicking the misspecifications researchers might make in practice. This deliberate violation of the sequential ignorability assumption ensures poor model fit, creating conditions to detect misspecifications. Second, I apply a univariate LM test to identify the top 25 candidate parameters ranked by LM chi-square statistics and Expected Parameter Change (EPC) values, excluding those with small EPCs, violations of temporal ordering, or potential non-identification problems in the RI-CLPM. Third, I refine the model using a forward stepwise Wald test, retaining only parameters with

$p < 0.05$ while removing any that cause convergence issues, non-positive definite covariance matrices, or negative variances. Identified parameters suggest possible latent confounders, which I incorporate into an extended RI-CLPM to assess their effect on autoregressive and cross-lagged coefficients. Substantial changes imply bias from unmeasured confounding, whereas stability increases confidence in the model's robustness. This procedure—combining LM-driven detection with Wald-based parsimony—offers a structured, scalable approach to sensitivity analysis for SEM-based panel models and can be implemented in R using *lavaan*.

4 LM Test & Wald Test

The LM test is a widely used diagnostic tool in SEM to assess whether freeing constrained parameters would improve model fit—often used to detect potential omitted paths. Formally, given a model with q free parameters and r constraints ($r < q$), the LM statistic evaluates whether any constrained parameters should be freed. When variables are continuous and normally distributed, the LM statistic is derived from the maximum likelihood fit function:

$$F(\theta) = \log|\Sigma(\theta)| - \log|S| + \text{tr}(S\Sigma(\theta)^{-1}) - p. \quad (7)$$

Let $\hat{\theta}$ be a vector of constrained estimators of θ constraints $h(\theta)=0$ when minimizing the fit function $F(\theta)$. With r constraints, there exists an $r \times 1$ constraint vector $h(\theta)' = (h_1, \dots, h_r)$. When minimizing the fit function $F(\theta)$ subject to the constraint $h(\theta)=0$, matrices of derivatives $\mathbf{g} = (\frac{\partial F}{\partial \theta})$ and $\mathbf{L}' = (\frac{\partial h}{\partial \theta})$ exist, and a vector of LM λ can be defined such that:

$$\hat{\mathbf{g}} + \hat{\mathbf{L}}'\hat{\lambda} = 0 \text{ and } h(\hat{\theta}) = 0. \quad (8)$$

In the context of constraints, the asymptotic covariance matrix can be derived from a matrix based on \mathbf{H} , augmented by the matrix of derivatives \mathbf{L} and a null matrix \mathbf{O} . Thus, the sample variance covariance matrix of the estimated parameter $\sqrt{n}(\hat{\boldsymbol{\theta}} - \boldsymbol{\theta})$ is given by the inverse of the information matrix of $\mathbf{H}(\boldsymbol{\theta})$ in the case of maximum likelihood estimation, and \mathbf{R} gives the covariance matrix of the Lagrange multipliers $\sqrt{n}(\hat{\boldsymbol{\lambda}} - \boldsymbol{\lambda})$, which is derived from the inverse of the information matrix \mathbf{L} . Hence, we can define

$$\begin{bmatrix} \mathbf{H} & \mathbf{L}' \\ \mathbf{L} & \mathbf{O} \end{bmatrix}^{-1} = \begin{bmatrix} \mathbf{H}^{-1} - \mathbf{H}^{-1}\mathbf{L}'(\mathbf{LH}^{-1}\mathbf{L}')^{-1} & \mathbf{H}^{-1}\mathbf{L}'(\mathbf{LH}^{-1}\mathbf{L}')^{-1} \\ (\mathbf{LH}^{-1}\mathbf{L}')^{-1}\mathbf{LH}^{-1} & -(\mathbf{LH}^{-1}\mathbf{L}')^{-1} \end{bmatrix} = \begin{bmatrix} \mathbf{M} & \mathbf{T}' \\ \mathbf{T} & -\mathbf{R} \end{bmatrix}. \quad (9)$$

Under regularity conditions and the null hypothesis $\mathbf{H}(\boldsymbol{\theta})$, the LM test statistics are asymptotically distributed as a χ^2 variate with $r \, df$. When testing a single constraint, the univariate LM statistic follows a χ^2 variate with 1 df . This makes the test particularly useful for evaluating whether a specific parameter in the $\boldsymbol{\theta}_r$ vector is equal to 0:

$$T_{LMi} = n\hat{\boldsymbol{\lambda}}_i' \hat{\mathbf{R}}_{ii}^{-1} \hat{\boldsymbol{\lambda}}_i \sim \chi_{r1}^2. \quad (10)$$

4.1 Expected Parameter Change (EPC)

The LM test provides the expected parameter change (EPC) score, which estimates how much a fixed or constrained parameter would shift if freely estimated. Researchers commonly use the LM test with EPCs to identify potential model modifications and unmeasured confounders in SEM. Oberski (2014), for instance, used EPC to evaluate the sensitivity of substantive parameters to violations of measurement invariance. The EPC approximates the expected change in parameters of interest when cross-group invariance constraints are relaxed, demonstrating how unaccounted measurement differences could confound substantive conclusions. In this study, I use EPCs as a form of local sensitivity analysis to examine whether fixed structural paths significantly influence model estimates.

Based on the statistical framework of the LM test in Equation 10, the univariate EPC for a fixed parameter can be expressed as

$$EPC_i = \hat{\lambda}_i / \hat{\mathbf{R}}_{ii}. \quad (11)$$

The subscript indicates evaluation at the constrained estimate. While a particular parameter may change when the constraint is released, its effects can be assessed across all constraint equations to identify which constraints may be worth relaxing (Chou & Bentler, 1993).

Large EPCs indicate potential overconstraints in the model. This issue is especially pronounced with small samples, where the LM test's effectiveness is diminished and more vulnerable to random fluctuations (MacCallum et al., 1992; Yuan & Liu, 2021). Moreover, LM test performance is shaped by sample size, df , and model complexity. The LM test assesses all possible paths based on the model's df ; while more df raise the risk of detecting spurious paths—especially when few are truly omitted—this risk decreases with larger sample sizes (Zheng & Bentler, 2025).

4.2 The Wald Test

The Wald test statistic complements the LM test and is calculated as follows:

$$W = n\hat{\boldsymbol{\theta}}_r'(\hat{\mathbf{L}}\hat{\mathbf{H}}^{-1}\hat{\mathbf{L}}')\hat{\boldsymbol{\theta}}_r \sim \chi_r^2, \quad (12)$$

where $\hat{\mathbf{L}}$ is a quadratic form, larger values indicate stronger evidence against the null. The univariate Wald statistic $\hat{\boldsymbol{\theta}}_i$ for each parameter in $\hat{\boldsymbol{\theta}}_r$ can be computed as

$$W_i = n\hat{\boldsymbol{\theta}}_i'\hat{\mathbf{H}}_{ii}^{-1}\hat{\boldsymbol{\theta}}_i = n\boldsymbol{\theta}_i^2/\hat{\mathbf{H}}_{ii} \sim \chi_i^2, \quad (12)$$

where $\hat{\theta}_i$ is one of the parameters in $\hat{\theta}_r$ and \hat{H}_{ii} is the i th parameter in the diagonal of the H matrix. The Wald test uses a stepwise procedure, beginning with the parameter that has the smallest test statistic. Parameters with $p < 0.05$ are retained, and the process continues until all have been evaluated.

5 Monte Carlo Simulation

This simulation study involves three main steps. In the first step, I generate simulated data from three distinct RI-CLPMs, which serve as our population models. The data generation follows the RI-CLPM covariance matrix structure (see Appendix). Specifically, a p -dimensional variable, \mathbf{z}_i , is generated as $\mathbf{z}_i = \mathbf{\Sigma}(\boldsymbol{\theta})^{1/2} \boldsymbol{\varepsilon}_i$, where $\mathbf{\Sigma}(\boldsymbol{\theta})$ is the covariance matrix. The vector $\boldsymbol{\varepsilon}_i \sim N(0, 1)$ represents random errors drawn from a standard multivariate normal distribution with zero mean and identity variance. For the parameter values, I set AR parameters β_{xi} and CL parameters γ_{yi} at 0.25 and 0.15 respectively. I use the same parameter values and specifications for the time-varying component of the RI-CLPM across all models to ensure comparability and validate the simulation results. Although parameter choices in simulations can be arbitrary, they do not affect test statistics or fit indices when models are correctly specified. In the second step, I specify three analysis models that deliberately omit confounders influencing the independent and outcome variables. In the third step, I apply both the LM and Wald tests to detect these omitted confounders and compare their effectiveness. All data generation simulations are performed in R using the lavaan package (Rosseel, 2012).

5.1 Population Models

Each population model is a four-wave RI-CLPM with two latent variables—X and Y—measured by single indicators at each time point. The RI-CLPM structure separates within-person fluctuations (e.g.,

deviations from one's mean trajectory) from stable between-person differences. To increase complexity while avoiding overfitting, I use four time points rather than more indicators per construct.

Figure 2. Diagram of Population Models

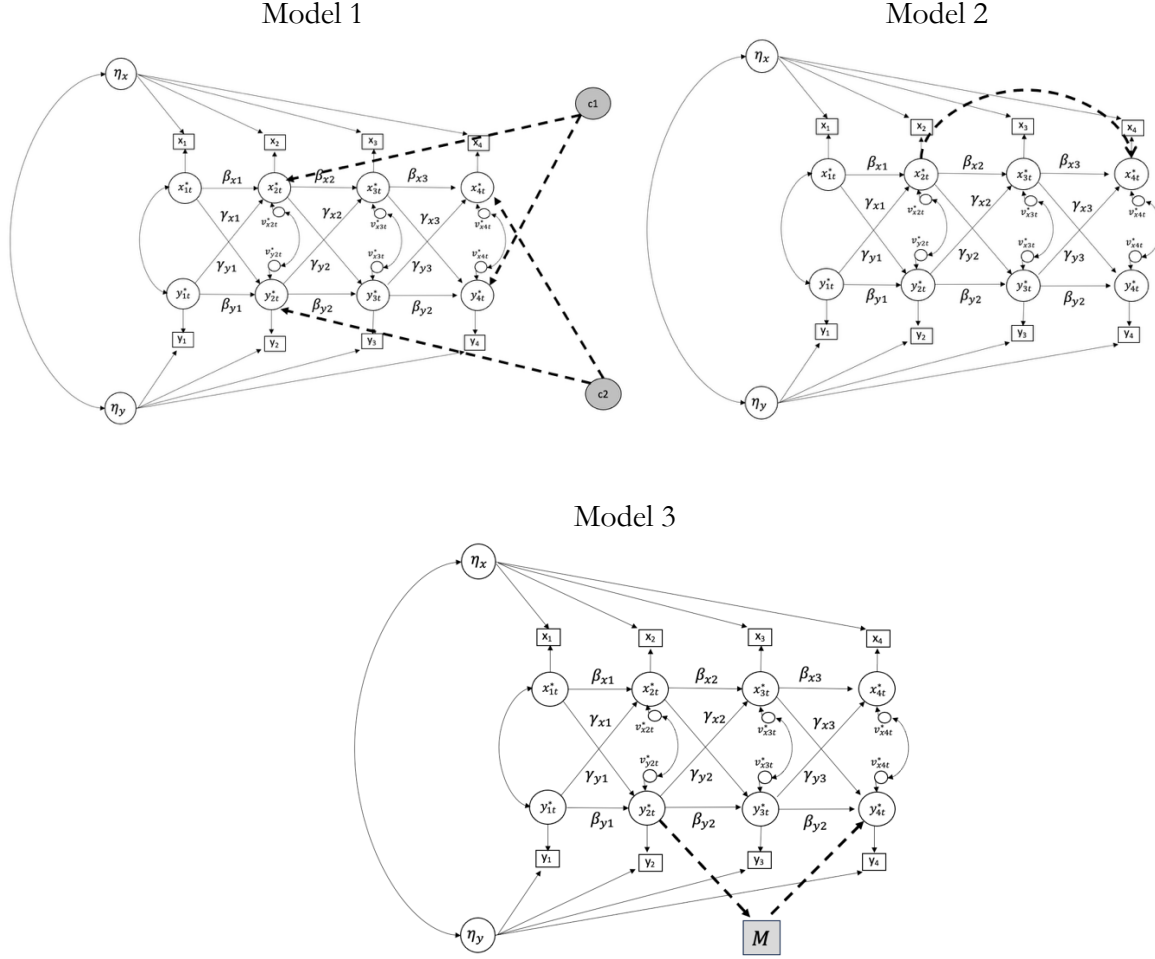


Figure 2 presents diagrams of three RI-CLPMs that share a common baseline structure but differ in their unmeasured confounding designs. Each model is based on a four-wave RI-CLPM framework that includes both within-person and between-person components. For the within-person component, two sets of latent variables, x_{it}^* and y_{it}^* , for $i = 1, 2, \dots, 4$, are specified. Each latent variable is measured by a single observed indicator, x_i and y_i , respectively. For the between-person component,

two latent factors, η_x and η_y are introduced to capture stable individual traits. Additionally, η_x and η_y are allowed to correlate, reflecting the association between stable traits across constructs.

Model 1 introduces two higher-order latent confounders, c_1 and c_2 , representing dynamic confounding between the residuals of x_{2t}^* and y_{4t}^* , and between the residuals of y_{2t}^* and x_{4t}^* , respectively. For example, in political communication, c_1 could capture unobserved partisan media exposure that simultaneously influences political efficacy and later policy support, while c_2 might reflect unmeasured interpersonal political discussion affecting earlier policy support and later efficacy. By inducing correlated residual variation across time and constructs, these confounders can bias cross-lagged path estimates.

Model 2 imposes a unidirectional direct path from x_{2t}^* to x_{4t}^* , representing a case where an earlier latent variable exerts a causal influence on a later one while bypassing intermediate processes. In political behavior terms, this could capture citizens' trust in government at time t directly shaping trust at $t + 2$, without accounting for mediating influences such as media exposure or political events. This specification violates temporal stationarity by assuming the effect remains constant across time, thereby conflating transient causal effects with stable dispositions or prior attitudes.

Model 3 incorporates unmeasured confounding within a mediation framework, where the residual of y_{2t}^* on the residual of y_{4t}^* indirectly through the residual of an unobserved mediator M , which itself is regressed on x_1 . For example, political engagement could mediate the relationship between political efficacy at two time points. Omitting M risks misattributing mediated effects as direct effects, thereby biasing causal interpretations. In sum, all three models intentionally violate the sequential ignorability assumption central to causal mediation analysis. Simulated data from these population models are then analyzed using deliberately misspecified analysis models that omit the latent confounders or structural paths, producing the expected model misfit.

The simulation focuses on latent variable correlations and regressions with fixed factor loadings (set to 1), isolating time-varying effects. Correlations among between-person traits and with other variables are excluded due to fixed loadings implying no residual variance at this level. To assess generalizability, additional analyses of 5-wave RI-CLPM with two indicators, and conventional CLPM are included in the Appendix.

5.2 Baseline Model Specification and Validity

Parameter estimation, model fit, and sensitivity analysis all depend on correct model specification. Before conducting simulations on the three variants, it is crucial to verify that both the baseline population model and the analysis model meet the necessary asymptotic assumptions—that is, how an estimator behaves as the sample size approaches infinity, typically converging in probability to the true parameter, thus providing a theoretical basis for inference when finite-sample behavior is uncertain. To achieve this, I evaluate the model fit across repeated samples with varying sample sizes. If a model is identified and adequately specified, we expect the model to follow a standard χ^2 distribution, $T_{ML} \xrightarrow{\mathcal{L}} \chi^2_{df}$, as sample size grows larger, demonstrating asymptotic properties (Bentler & Dijkstra, 1985; Browne, 1984; Jöreskog & Sörbom, 1988). Accordingly, I use Monte Carlo simulation to generate data from the predefined population models and estimate the corresponding analysis models using the simulated data.

Table 1. Monte Carlo simulation and Asymptotic property of RI-CLPM population model

N	Chi-square	SD	P-value	Rej Rate	NFI	CFI	RMSEA
100	9.214	4.402	0.490	0.068	0.937	0.959	0.119
200	9.195	4.170	0.486	0.058	0.985	1.000	0.000
300	9.178	4.381	0.491	0.050	0.991	1.000	0.000
500	8.909	4.472	0.513	0.056	0.991	0.998	0.028
800	9.034	4.380	0.501	0.060	0.997	1.000	0.000
1000	9.018	4.140	0.495	0.042	0.999	1.000	0.000
5000	9.138	4.116	0.484	0.040	1.000	1.000	0.000
10000	8.921	4.546	0.513	0.050	1.000	1.000	0.006

Note: Expected chi-square is 9, SD=4.24, P -value=0.5, rejection rate=0.05.

The Monte Carlo simulations in this study were based on population model. I conducted 500 trials and calculated the average statistics, which are reported in Table 1. I examined the performance of the analysis model by varying the sample sizes from 100 to 10,000. Since the simulated data were normally distributed, the maximum likelihood estimator was sufficient to examine the basic statistical performance and asymptotic properties. Table 1 presents the average χ^2 test statistics, standard deviations, p -values, rejection rates, and fit indices (NFI, CFI, RMSEA) by sample size. As shown in Table 1, as the sample size increases, all mean statistics test statistics get closer to the expected values: $\chi^2=9$, SD=4.24, p -value=0.50, and empirical rejection rate is 0.05. In addition, NFI and CFI become closer to 1, and RMSEA is about 0 when the sample sizes are greater than 200. Naturally, with smaller sample sizes, test statistics and fit indices deviate from their expected values—a well-documented issue for the maximum likelihood estimator (Zheng & Bentler, 2021, 2023, 2024). The collective statistical indicators demonstrate that the population and baseline analysis models are well-specified. Based on this baseline model, I will proceed with various analyses.

6 The Two-Stage Process for Confounder Searches

6.1 *Stage One: Selection of Testing Parameters*

I start with a univariate LM test to identify the top candidate parameters based on their LM chi-square statistics and EPC values. I select the top 25 parameters from this test but exclude any that violate the following criteria:

1. Parameters that contradict temporal ordering (e.g., a variable at time t predicting one at $t-1$) or conflict with the population model (e.g., LM-suggested correlations between autoregressively linked latent variables or fixed variances). In RI-CLPMs, suggestions linking latent variables to their indicators, which may cause non-identification or convergence problems, are also excluded.

2. Parameters that introduce redundant or meaningless relations, such as correlations between autoregressive and cross-lagged paths, are removed.
3. Parameters with extremely small EPC values are excluded.
4. Finally, I add the remaining candidate parameters one at a time to the analysis model; any parameter that causes convergence or identification issues is removed.

6.2 *Stage Two: Wald Test*

The Wald test follows, assessing candidate parameters identified by the LM test through a forward stepwise procedure. Each parameter is added individually, and the Wald statistic and p -value are computed at each step. This process continues until all candidates are evaluated, enhancing model parsimony and reducing false positives from overfitting. Ultimately, only parameters with p -values below 0.05 are retained for further analysis.

6.3 *Simulation Result*

Tables 2–4 report Monte Carlo simulation results. Latent constructs WFX and WFY are measured at multiple time points (e.g., WFX1, WFX2). Significant Wald test results align with the population model. LM tests successfully flag confounders via large chi-square statistics and EPC values; Wald tests confirm true effects and reject false ones. Estimated AR and CL paths match the population parameters (see Table A1 in the Appendix). Simulations with more complex models—featuring higher-order latent variables, additional waves, and multiple indicators—are also included in the Appendix and show similarly robust performance.

Table 2. Model 1 (Correlation) Simulation Result

		Chi-square	EPC	Wald Test	p-value
WFX4 ~	WFY2	575.299	0.447	12.780	0.000
WFX4 ~	WFY2	561.970	0.810	0.537	0.464
WFX2 ~	WFY4	540.303	0.419	7.874	0.005
WFY4 ~	WFX2	515.640	0.764	0.372	0.796
WFY4 =	X2	499.933	0.642	0.481	0.488

Table 3. Model 2 (Direct Effect) Simulation Result

		Chi-square	EPC	Wald Test	P-value
WFX4	~ WFX2	222.566	1.142	5.547	0.019
WFX4	~~ WFX3	196.282	-0.110	0.528	0.467
WFX4	=~ y3	190.300	-1.024	1.278	0.258
WFX4	=~ x2	172.917	0.458	0.049	0.824

Table 4. Model 3 (Mediation) Simulation Result

			Chi-square	EPC	Wald Test	P-value
WFX4	~ c1		285.407	0.742	20.932	0.000
WFX4	~ WFX2		183.201	1.578	5.117	0.024
WFX4	=~ y3		148.494	1.367	0.546	0.460
WFX1	~ x1		143.828	-2.882	0.115	0.735
WFX2	~~ WFX4		138.537	0.079	0.065	0.799
WFX4	=~ y2		132.760	0.447	3.844	0.050
WFX4	~ x1		116.008	0.416	0.387	0.534

Note: I follow the same notation conventions used in lavaan, where =~ denotes a latent variable definition, ~ indicates a regression relationship, and ~~ represents a covariance or correlation.

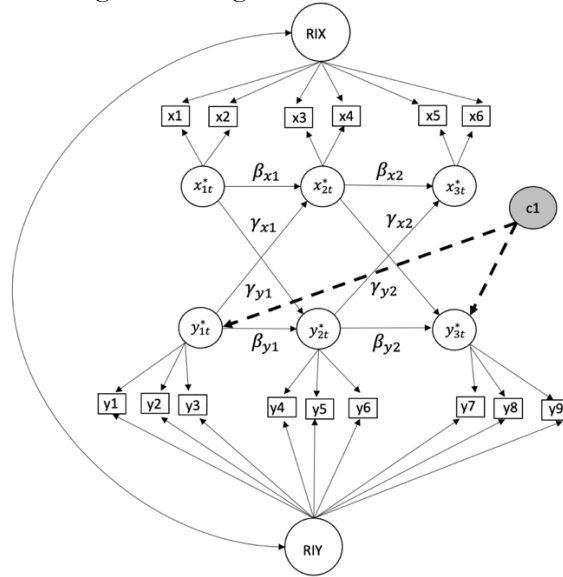
7 Empirical Application

This section presents an empirical example that demonstrates the flexibility of the 2SLW approach and illustrates its application within a RI-CLPM framework. Beyond showcasing the 2SLW method, this example also aims to encourage the broader adoption of RI-CLPM in political behavior research, where its use remains relatively limited. To this end, I apply the RI-CLPM to data from the Longitudinal Internet Studies for the Social Sciences (LISS) panel—a long-term, internet-based survey of individuals and households in the Netherlands, administered by CentERdata. Building on Bakker et al.’s (2021) “Reconsidering the Link Between Self-Reported Personality Traits and Political Preferences”, I construct a three-wave panel using data collected in 2008, 2014, and 2020. The RI-CLPM allows us to separate stable individual differences from within-person fluctuations over time as I examine how agreeableness influences attitudes toward immigration.

Agreeableness is measured using two items: (1) “Interested in people” and (2) “I am not interested in other people’s problems” (reverse coded). Immigration attitudes are assessed using three items: (1) “There are too many people of foreign origin or descent in the Netherlands,” (2) “Legally residing

foreigners should be entitled to the same social security as Dutch citizens,” and (3) “It should be made easier to obtain asylum in the Netherlands.” Responses are recorded on a five-point Likert scale ranging from “fully disagree” to “fully agree.” Our analytic strategy is twofold. First, I estimate the causal relationship between agreeableness and immigration attitudes using a standard RI-CLPM. Next, I apply the 2SLW approach to detect potential unmeasured confounders that may bias the estimates. I then compare the goodness-of-fit statistics, fit indices, and the AR and CL coefficient estimates between the baseline model and the model adjusted using the 2SLW approach.

Figure 4. Diagram of the RI-CLPM



The agreeableness and political attitude items are denoted as X_i and Y_i , respectively in Figure 4. To examine the effects of agreeableness on immigration attitudes, I construct a series of latent variables, x_{it}^* and y_{it}^* , measured by agreeableness and political attitude items across the 2008, 2014, and 2020 waves. The parameters β_{xi} and β_{yi} represent AR effects, while γ_{xi} and γ_{yi} denote CL effects. The dashed lines connecting the latent variable c_1 to y_{1t}^* and y_{3t}^* indicate confounding paths identified by the 2SLW approach.

Table 6. The 2SLW Test Result

			Chi-square	EPC	Wald Test	P-value
WFY1	~~	WFY3	53.615	0.143	15.464	0.000
WFY3	=~	Immigrant Benefits'08	43.627	0.679	1.596	0.207
WFX1	~~	WFY3	40.390	-0.244	0.593	0.441
WFY2	=~	Immigrant Benefits'08	38.387	0.969	4.862	0.027

Table 6 presents the results of the LM and Wald tests. The LM test identified four parameters, of which only two were statistically significant according to the Wald test, as highlighted. Notably, the correlation between WFY1 and WFY3 yielded the largest chi-square value and the highest Wald test statistic, indicating strong statistical significance. These two parameters will be incorporated into the existing model.

Table 7. AR & CL Coefficients of Original and Improved Models

Original Model				Improved Model				Difference
	Estimate	Std. Err	P-value		Estimate	Std. Err	P-value	
WFX2 ~				WFX2 ~				
WFX1	0.824	0.031	0.000	WFX1	0.825	0.027	0.000	0.001
WFY1	0.121	0.160	0.450	WFY1	-0.096	0.016	0.010	-0.217
WFY2 ~				WFY2 ~				
WFY1	1.585	0.185	0.000	WFY1	0.977	0.023	0.000	-0.608
WFX1	0.047	0.024	0.049	WFX1	-0.025	0.025	0.026	-0.072
WFX3 ~				WFX3 ~				
WFX2	0.961	0.030	0.000	WFX2	0.906	0.029	0.000	-0.055
WFY2	0.089	0.081	0.268	WFY2	0.006	0.015	0.854	-0.083
WFY3 ~				WFY3 ~				
WFY2	1.015	0.076	0.000	WFY2	0.861	0.071	0.000	-0.154
WFX2	-0.071	0.021	0.001	WFX2	-0.051	0.081	0.136	0.020
				C1=~				
				WFY1	0.584			
				WFY3	0.180	0.143	0.028	
Model Fit								
Chi-square	679.509				130.809			-548.700
DF	74				65			-9.000
CFI	0.991				1.000			0.009
NFI	0.990				0.998			0.008
TLI	0.988				1.000			0.012
RMSEA	0.059				0.011			-0.048

Note: All coefficients are standardized

Table 7 compares the AR and CL coefficients from the original and improved models. In the original model, the cross-lagged paths from WFX2 to WFY1 and from WFY2 to WFX1 are statistically significant but run in an unexpected direction. This anomaly likely reflects model misspecification,

supported by a poor chi-square statistic of 679.509 ($df=74$). The model also exhibits a negative variance estimate, further underscoring the misspecification despite acceptable fit indices.

In sharp contrast, the improved model produces more consistent and theoretically appropriate cross-lagged estimates. While the path from WFX3 to WFY2 is not statistically significant, most other parameters are stable and interpretable—that is, they align with findings in the political psychology literature. In particular, stronger agreement with empathetic concern for others is generally associated with reduced support for exclusionary statements (Batson et al., 2002; Simas et al., 2019; Sirin et al., 2021). Although modest, the latent confounder $c1$ —with factor loadings of 0.584 and 0.180, respectively—induces a correlation just above 0.10. Even this small degree of confounding can bias the estimated causal effect and obscure its substantive interpretation.

Importantly, the improved model demonstrates substantially better fit, as reflected by a chi-square value of 130.809 ($df=65$). Other fit indices—CFI, NFI, TLI, and RMSEA—also indicate excellent fit. Taken together, Tables 6 and 7 provide strong evidence that the improved model offers a significantly better fit to the data than the original specification. Without identifying the unmeasured confounder, the substantive conclusions about the causal effects—and the arguments built upon them—could have been misleading.

8 Discussion & Conclusion

Rigorous investigation of causal effects is fundamental to social and behavioral research, necessitating a diverse set of analytical tools. While panel models are powerful for causal inference with observational data, unobserved confounding continues to pose a significant challenge. This study has introduced the 2SLW approach as a diagnostic tool for identifying potential confounders within the RI-CLPM framework. Through Monte Carlo simulations, I evaluated the method under three

scenarios of confounding: distortion of the (1) predictor-outcome association, (2) direct effect, and (3) mediation pathway. I further demonstrated its practical utility through an empirical application. While simulations cannot capture every real-world complexity, results from the RI-CLPM and CLPM demonstrate that the 2SLW approach is effective and scalable. Its design also supports generalization to other SEM-based panel models and extended panel structures.

In light of this, the study offers three key contributions. First, it extends the LM test to panel causal models, such as the RI-CLPM, enabling a more systematic and less subjective assessment of unmeasured confounding in sensitivity analysis. Second, these methodological advancements improve the reliability of inferences drawn from complex longitudinal panel data by providing stronger diagnostic tools to detect unmeasured confounders in a wide range of applied settings. Third, by improving detection of unmeasured confounding, the approach strengthens causal inference in social and behavioral sciences using SEM panel data.

As others have emphasized, any model modification or sensitivity analysis must be grounded in theory and cross-validation to guard against overfitting. The 2SLW test is no exception. It serves as a data-driven guide for uncovering potential confounding but should be interpreted as exploratory rather than prescriptive. Ultimately, the decision to modify models or add parameters must rest on theoretical justification. While this study focuses on detection, future research could build on this work by integrating formal sensitivity analysis frameworks to estimate the potential impact of unmeasured confounding on causal parameters.

References

- Acharya, A., Blackwell, M., & Sen, M. (2016). Explaining Causal Findings Without Bias: Detecting and Assessing Direct Effects. *American Political Science Review*, 110(3), 512-529. <https://doi.org/doi:10.1017/S0003055416000216>
- Bakker, B., Lelkes, Y., & Malka, A. (2021). Reconsidering the Link Between Self-Reported Personality Traits and Political Preferences. *American Political Science Review*, 115(4), 1482-1498. <https://doi.org/doi:10.1017/S0003055421000605>
- Bakker, B., Schumacher, G., & Rooduijn, M. (2021). Hot politics? Affective responses to political rhetoric. *American Political Science Review*, 115(1), 150-164.
- Batson, C. D., Chang, J., Orr, R., & Rowland, J. (2002). Empathy–Attitudes–Action Framework in Social Psychology. *Personality and Social Psychology Bulletin*, 28(12), 1656-1666. <https://doi.org/https://doi.org/10.1177/014616702237647>
- Bentler, P. M., & Dijkstra, T. (1985). Efficient Estimation via Linearization in Structural Models. In P. R. Kirshnaiah (Ed.), *Multivariate Analysis VI* (pp. 9-42). North-Holland.
- Blackwell, M. (2014). A Selection Bias Approach to Sensitivity Analysis for Causal Effects. *Policy Analysis*, 22, 169-182.
- Browne, M. (1984). Asymptotically distribution-free methods for the analysis of covariance structures. *British Journal of Mathematical and Statistical Psychology*, 37, 62-83. <https://doi.org/doi:10.1111/bmsp.1984.37.issue-1>
- Bullock, J. G., Green, D., & Ha, S. E. (2010). Yes, But What's the Mechanism? (Don't Expect an Easy Answer). *Journal of Personality and Social Psychology*, 98(4), 550-558.
- Chiu, A., Lan, X., Liu, Z., & Xu, Y. (2025). ausal Panel Analysis under Parallel Trends: Lessons from a Large Reanalysis Study. *American Political Science Review*, 1-22. <https://doi.org/https://doi.org/10.1017/S0003055425000243>
- Chou, C.-P., & Bentler, P. M. (1993). Invariant Standardized Estimated Parameter Change for Model Modification in Covariance Structure Analysis. *Multivariate Behavioral Research*, 28(1), 97-110. https://doi.org/https://doi.org/10.1207/s15327906mbr2801_6
- Dinesen, P. T., Sonderskov, K. M., Sohlberg, J., & Esaiasson, P. (2022). Close (Causally Connected) Cousins? Evidence on the Causal Relationship between Political trust and Social Trust *Public Opinion Quarterly*, 86(3), 708-721. <https://doi.org/https://doi.org/10.1093/poq/nfac027>
- Feldman, S., Panish, A., Weber, C., & Zheng, B. Q. (2025). *Rethinking the Cross Lagged Regression Model: Limitations and Alternatives in Panel Analysis* MPSA, Chicago.
- Goren, P. (2005). Party Identification and Core Political Values. *American Journal of Political Science*, 49(4), 882-897.
- Hamaker, E. L., Kuiper, R. M., & Grasman, R. P. P. P. (2015). A critique of the cross-lagged panel model. *Psychological Methods*, 20, 102-116.
- Harring, J. R., McNeish, D. M., & Hancock, G. R. (2017). Using Phantom Variables in Structural Equation Modeling to Assess Model Sensitivity to External Misspecification. *Psychol Methods*, 22(4), 616-631. <https://doi.org/https://doi.org/10.1037/met0000103>
- Hatemi, P. K., Crabtree, C., & Smith, K. (2019). Ideology Justifies Morality: Political Beliefs Predict Moral Foundations. *American Journal of Political Science*, 63(4), 788-806. <https://doi.org/DOI:10.1111/ajps.12448>
- Hayakawa, K. (2019). Corrected Goodness-of-fit test in covariance structure analysis. *Psychological Methods*, 24(3), 371-389.
- Holland, P. W. (1988). Causal Inference, Path Analysis, and Recursive Structural Equations Models. *Sociological Methodology*, 18, 449-484.

- Imai, K., Keele, L., & Tingley, D. (2010). A General Approach to Causal Mediation Analysis. *Psychol Methods*, 15(4), 309-326.
- Imai, K., Keele, L., Tingley, D., & Yamada, T. (2011). Unpacking the Black Box of Causality: Learning about Causal Mechanisms from Experimental and Observational Studies. *American Political Science Review*, 105(4), 765-789.
- Imai, K., Lo, J., & Olmsted, J. (2016). Fast Estimation of Ideal Points with Massive Data. *American Political Science Review*, 110(4), 631-656.
- Imai, K., Tingley, D., & Yamamoto, T. (2013). Experimental Designs for Identifying Causal Mechanisms. *Journal of the Royal Statistical Society. Series A (Statistics in Society)*, 176(1), 5-32.
- Jöreskog, K. G., & Sörbom, D. (1988). *LISREL 7, A Guide to the Program and Applications*. SPSS.
- Lucas, R. (2023). Why the Cross-Lagged Panel Model Is Almost Never the Right Choice. *Advances in Methods and Practices in Psychological Science*, 6(1), 1-22.
<https://doi.org/https://doi.org/10.1177/25152459231158>
- Luttig, M. D. (2021). Reconsidering the Relationship between Authoritarianism and Republican Support in 2016 and Beyond. *Journal of Politics*, 83(2), 783-787.
- MacCallum, R. C., Roznowski, M., & Nectowitz, L. B. (1992). Model Modifications Covariance Structure Analysis: The Problem of Capitalization on Chance. *Psychological Bulletin*, 111(3), 490-504.
- MacKinnon, D. P. (2008). *Introduction to Statistical Mediation Analysis*. Routledge.
- MacKinnon, D. P., & Pirlott, A. G. (2015). Statistical Approaches for Enhancing Causal Interpretation of the M to Y Relation in Mediation Analysis. *Personality and Social Psychology Review*, 19(1), 30-43.
- Mund, M., Johnson, M. D., & Nestler, S. (2021). Changes in Size and Interpretation of Parameter Estimates in Within-Person Models in the Presence of Time-Invariance and Time-Varying Covariate. *Frontiers in Psychology*.
<https://doi.org/https://doi.org/https://doi.org/10.3389/fpsyg.2021.666928>
- Pearl, J. (2001). Direct and Indirect Effects. In J. B. D. Koller (Ed.), *Proceedings of the Seventeenth Conference on Uncertainty in Artificial Intelligence* (pp. 411-420). Morgan Kaufmann Publishers Inc.
- Robins, J. M., & Greenland, S. (1992). Identifiability and Exchangeability for Direct and Indirect Effects. *Epidemiology*, 3(2), 143-155.
- Rosseel, Y. (2012). lavaan: An R package for structural equation modeling. *Journal of Statistical Software*, 48(2), 1-36.
- Simas, E. N., Clifford, S., & Kirland, J. H. (2019). How Empathic Concern Fuels Political Polarization. *American Political Science Review*, 114(1), 258-269.
<https://doi.org/https://doi.org/10.1017/S0003055419000534>
- Sirin, C. V., Valentino, N., & Villalobos, J. D. (2021). *Seeing Us in Them Social Divisions and the Politics of Group Empathy*. Cambridge University Press.
<https://doi.org/https://doi.org/10.1017/9781108863254>
- Usami, S. (2021). On the differences between general cross-lagged panel model and random-intercept cross-lagged panel model: Interpretation of cross-lagged parameters and model choice. *Structural Equation Modeling: A Multidisciplinary Journal*, 28(3), 331-344.
- Usami, S., Murayama, K., & Hamaker, E. L. (2019). A unified framework of longitudinal models to examine reciprocal relations. *Psychol Methods*, 24(5), 637-657.
- Yuan, K. H., & Liu, F. (2021). Which Method is More Reliable in Performing Model Modification: Lasso Regularization or Lagrange Multiplier Test? *Structural Equation Modeling: A Multidisciplinary Journal*, 28(1), 69-81.

- Zheng, B. Q., & Bentler, P. (2025). Improved LM Test for Robust Model Specification Searches in Covariance Structure Analysis: Application in Political Science Research. *Political Science Research & Methods*, 1-21. <https://doi.org/doi:10.1017/psrm.2025.27>
- Zheng, B. Q., & Bentler, P. M. (2021). Testing Mean and Covariance Structures with Reweighted Least Squares. *Structural Equation Modeling: A Multidisciplinary Journal*. <https://doi.org/https://doi.org/10.1080/10705511.2021.1977649>
- Zheng, B. Q., & Bentler, P. M. (2023). RGLS and RLS in Covariance Structure Analysis. *Structural Equation Modeling: A Multidisciplinary Journal*, 30(2), 234-244. <https://doi.org/https://doi.org/10.1080/10705511.2022.2117182>
- Zheng, B. Q., & Bentler, P. M. (2024). Enhancing Model Fit Evaluation in SEM: Practical Tips for Optimizing Chi-Square Tests. *Structural Equation Modeling: A Multidisciplinary Journal*(Advance online publication). <https://doi.org/https://www.tandfonline.com/doi/full/10.1080/10705511.2024.2354802>
- Zheng, B. Q., & Valente, M. J. (2023). Evaluation of Goodness-of-Fit Tests in Random Intercept Cross-Lagged Panel Model: Implications for Small Samples. *Structural Equation Modeling: A Multidisciplinary Journal*, 30(4), 604-617. <https://doi.org/https://doi.org/10.1080/10705511.2022.2149534>

Appendix

Table of Contents

The Covariance Matrix of the RI-CLPM.....	28
Monte Carlo simulation.....	30
Five-Wave RI-CLPM with Two Indicators Per Factor.....	30
Table A1. Monte Carlo and Asymptotic Results for 5-Wave RI-CLPM.....	31
Figure A1. 5-Wave RI-CLPM with 2 Indicators (Correlation).....	31
Table A2. Test Result for 5-Wave RI-CLPM with 2 Indicators (Correlation)	32
Table A3. AR & CL Effects – 5-Wave RI-CLPM (Correlation).....	33
Figure A2. 5-Wave RI-CLPM with 2 Indicators (Direct Effect)	34
Table A4. Test Result for 5-Wave RI-CLPM with 2 Indicators (Direct Effect)	34
Table A5. AR & CL Effects – 5-Wave RI-CLPM (Direct Effect)	35
Five-Wave RI-CLPM with Two Indicators Per Factor (Mediation)	35
Figure A3. 5-Wave RI-CLPM with 2 Indicators (Mediation).....	36
Table A6. Test Result for 5-Wave RI-CLPM with 2 Indicators (Mediation).....	36
Table A7. AR & CL Effects – 5-Wave RI-CLPM (Mediation).....	36
Cross-Lagged Panel Model (CLPM).....	38
Table A8. Monte Carlo and Asymptotic Results for CLPM	38
Figure A4. Diagram of CLPM (Correlation).....	39
Table A9. Test Result for CLPM (Correlation)	39
Table A10. AR & CL Effects for CLPM (Correlation).....	40
Cross-Lagged Panel Model—Direct Effect	41
Figure A5. Diagram of CLPM (Direct Effect).....	41
Table A11. Test Result for CLPM (Direct Effect).....	41
Table A12. AR & CL Effects for CLPM (Direct Effect).....	42
Cross-Lagged Panel Model—Mediation.....	42
Figure A6. Diagram of CLPM (Mediation)	43
Table A13. Test Result for CLPM (Mediation)	43
Table A14. AR & CL Effects for CLPM (Mediation)	44

This Appendix provides additional and detailed statistical tests to evaluate the performance of the 2SLW method, which could not be included in the main text due to space constraints. The R code and data will be available on the author's GitHub repository.

The Covariance Matrix of the RI-CLPM

In covariance structure analysis, the RI-CLPM can be expressed through its covariance matrix.

Specifically, Equations (5) and (6) can be reformulated in matrix form as follows:

$$\mathbf{z}_{it} = \boldsymbol{\delta}_i + \boldsymbol{\Phi} \mathbf{z}_{i(t-1)}^* + \boldsymbol{\eta}_i + \mathbf{v}_{it}, \quad (i = 1, \dots, n, t = 1, \dots, T) \quad (\text{A1})$$

$$\mathbf{z}_{i1} = \boldsymbol{\delta}_i + \boldsymbol{\Psi} \boldsymbol{\eta}_i + \boldsymbol{\varepsilon}_{i1}, \quad (i = 1, \dots, n) \quad (\text{A2})$$

where

$$\mathbf{z}_{it} = \begin{bmatrix} x_{it} \\ y_{it} \end{bmatrix}, \boldsymbol{\Phi} = \begin{bmatrix} \beta_x & \gamma_x \\ \beta_y & \gamma_y \end{bmatrix}, \boldsymbol{\eta}_i = \begin{bmatrix} \eta_{xi} \\ \eta_{yi} \end{bmatrix}, \mathbf{v}_i = \begin{bmatrix} v_{xit} \\ v_{yit} \end{bmatrix}, \boldsymbol{\delta}_i = \begin{bmatrix} \delta_{xi} \\ \delta_{yi} \end{bmatrix},$$

$$\boldsymbol{\Psi} = \begin{bmatrix} \psi_{11} & \psi_{12} \\ \psi_{21} & \psi_{22} \end{bmatrix}, \boldsymbol{\varepsilon}_{i0} = \begin{bmatrix} \varepsilon_{i0}^y \\ \varepsilon_{i0}^x \end{bmatrix}. \quad (\text{A3})$$

Building on the CLPM covariance matrix formulation in Hayakawa (2019), I assume that the largest eigenvalue of $\boldsymbol{\Phi}$ is less than 1, ensuring that \mathbf{z}_{it} follows a stable process. Using these matrices, I combine Equations (5) and (6) to obtain:

$$\mathbf{B} \mathbf{z}_i = \boldsymbol{\delta}_i + \mathbf{J} \boldsymbol{\pi}_i + \mathbf{u}_i, \quad (\text{A4})$$

where

$$\mathbf{B} = \begin{bmatrix} \mathbf{I}_2 & \mathbf{0} & \cdots & \mathbf{0} \\ -\mathbf{\Phi} & \mathbf{I}_2 & \cdots & \vdots \\ \vdots & \ddots & \ddots & \mathbf{0} \\ \mathbf{0} & \mathbf{0} & -\mathbf{\Phi} & \mathbf{I}_2 \end{bmatrix}, \quad (\text{A5})$$

$$\mathbf{\Gamma} = \mathbf{B}^{-1} = \begin{bmatrix} \mathbf{I}_2 & \mathbf{0} & \cdots & \mathbf{0} \\ \mathbf{\Phi} & \mathbf{I}_2 & \cdots & \vdots \\ \vdots & \ddots & \ddots & \mathbf{0} \\ \mathbf{\Phi}^{T-1} & \mathbf{0} & \mathbf{\Phi} & \mathbf{I}_2 \end{bmatrix}, \quad (\text{A6})$$

$$\mathbf{z}_{it} = \begin{bmatrix} z_{i1} \\ z_{i2} \\ \vdots \\ z_{iT} \end{bmatrix}, \quad \mathbf{u}_i = \begin{bmatrix} \varepsilon_{i1} \\ v_{i2} \\ \vdots \\ v_{iT} \end{bmatrix}, \quad (\text{A7})$$

$$\mathbf{J} = \begin{bmatrix} 1 & \mathbf{\Psi} \\ 0 & \mathbf{I}_2 \end{bmatrix}, \quad \boldsymbol{\pi}_i = \begin{bmatrix} \delta_i \\ \boldsymbol{\eta}_i \end{bmatrix}, \quad (\text{A8})$$

$$\mathbf{z}_i = \mathbf{\Gamma}(\mathbf{J}\boldsymbol{\pi}_i + \mathbf{u}_i). \quad (\text{A9})$$

Thus, we assume that $\boldsymbol{\pi}_i \sim (0, \boldsymbol{\Sigma}_\pi)$, $v_{it} \sim (0, \boldsymbol{\Sigma}_v)$, $\varepsilon_{i0} \sim (0, \boldsymbol{\Sigma}_\varepsilon)$, and δ_i , η_i , v_{it} , and ε_{i1} are uncorrelated, and each of them is independent and identically distributed. Therefore, the covariance matrix can be written as:

$$\boldsymbol{\Sigma}(\boldsymbol{\theta}) = \mathbf{\Gamma}(\mathbf{J}\boldsymbol{\Sigma}_\pi\mathbf{J}' + \boldsymbol{\Sigma}_u)\mathbf{\Gamma}' \quad (\text{A10})$$

where $\boldsymbol{\theta} = (\mathbf{\Phi}, \mathbf{\Psi}, \sigma_\pi^2, \sigma_v^2, \sigma_\varepsilon^2)'$, and $\boldsymbol{\Sigma}_u = \text{diag}(\sigma_\varepsilon^2, \sigma_v^2 \mathbf{I}_T)$.

Monte Carlo simulation

The data generation scheme for the simulation follows the covariance matrix of RI-CLPM as described earlier. In a normal distribution $\mathbf{z}_i = \mathbf{\Sigma}(\boldsymbol{\theta})^{1/2}\boldsymbol{\varepsilon}_i$, and the covariance matrix $\mathbf{\Sigma}(\boldsymbol{\theta})$ is drawn from a multivariate normal distribution with zero mean and unknown variance. $\boldsymbol{\varepsilon}_i$ follows a standard normal distribution $N(0, 1)$. For the parameter values, I set AR parameters β_{xi} and CL parameters γ_{yi} at 0.25 and 0.15 respectively. I use identical parameter values and specifications for the time-varying component of the RI-CLPM across all models, ensuring comparability and validation of the simulation results. Using identical parameter values in simulation facilitates validation and enables comparison with existing studies. While the choice of parameter values in simulations can be arbitrary, it does not affect test statistics or fit indices when models are correctly specified. Data generation can be implemented in R using the *lavaan* package.

Five-Wave RI-CLPM with Two Indicators Per Factor

To assess the flexibility of the 2SLW approach, I construct a more complex RI-CLPM featuring five waves of repeated measurements, where each latent factor is measured by two indicators. Additionally, I specify a second-order factor L , which is measured by the factors η_x and η_y . Following a similar strategy introduced in the main text, I design three scenarios: one in which the correlation between the two factors is driven by an unobserved latent confounder; another in which the association is modeled as a direct effect between the two factors; and a third in which the relationship follows a mediation path between two time-varying factors.

Prior to testing the three scenarios, I create a baseline model, which is based on Figure A1 but without those dash lines. As emphasized by previous studies, SEM-based panel models, including RI-CLPM, CLPM, latent growth models, etc. are based on parametric and asymptotic properties. That is,

they are linear and follow a distribution. Asymptotic properties refer to how an estimator or test behaves as the sample size approaches infinity, with key features like consistency—where the estimator converges in probability to the true parameter—providing theoretical justification for inference when finite-sample behavior is uncertain or complex.

Table A1. Monte Carlo and Asymptotic Results for 5-Wave RI-CLPM

N	Chi-square	SD	P-value	Rej Rate	NFI	CFI	RMSEA
100	186.332	19.895	0.273	0.215	0.841	0.993	0.020
200	177.391	18.738	0.389	0.101	0.922	1.000	0.000
300	175.550	18.554	0.415	0.078	0.945	1.000	0.000
500	172.176	19.222	0.472	0.070	0.960	0.997	0.011
800	172.169	19.271	0.469	0.068	0.974	0.997	0.012
1000	171.764	17.909	0.476	0.066	0.982	1.000	0.000
5000	171.068	18.024	0.490	0.062	0.996	1.000	0.003
10000	169.742	18.433	0.505	0.050	0.998	1.000	0.000

Note: Theoretically expected mean $\chi^2=170$, SD=18.44, P-value=0.5, rejection rate=0.05.

Figure A1. 5-Wave RI-CLPM with 2 Indicators (Correlation)

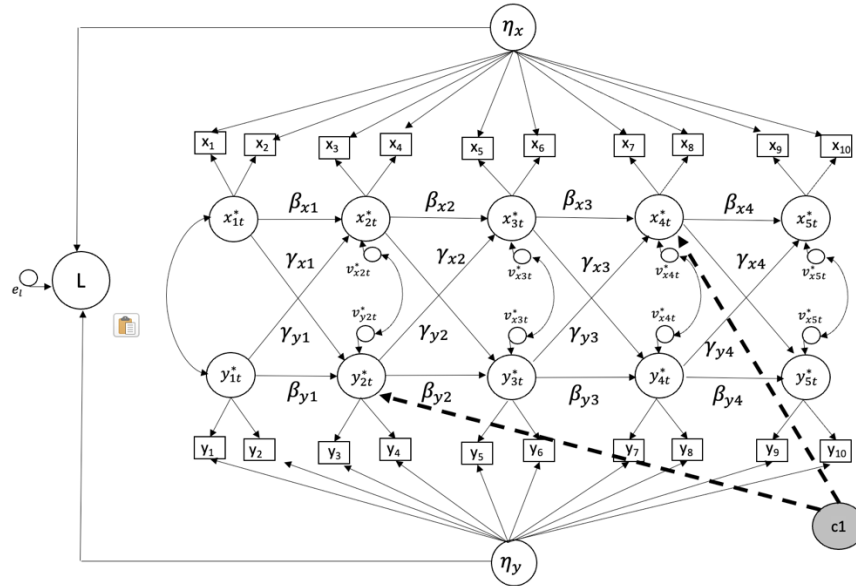


Table A2. Test Result for 5-Wave RI-CLPM with 2 Indicators (Correlation)

			LM χ^2	EPC	Wald Test	P-value
WFX4	~	WFX2	42.594	0.468	9.597	0.002
WFX5	~	WFX2	33.129	-0.337	1.839	0.175
WFX5	~~	WFX2	29.012	-0.374	0.676	0.411
WFX4	~	WFX1	12.763	-0.268	0.111	0.739
WFX4	=~	y22	8.778	0.141	0.616	0.433
WFX1	~~	WFX4	8.008	-0.236	0.010	0.920
WFX3	=~	x32	6.658	0.155	3.516	0.061
x31	~~	y32	6.190	-0.122	2.493	0.114

Figure A1 illustrates a hypothetical scenario where a latent confounder, c_1 affects the residuals of x_{4t}^* and y_{2t}^* . Using this specification, I generate a population model. I then estimate an analysis model that omits c_1 and its direct effects on the residuals of x_{4t}^* and y_{2t}^* . If the 2SLW approach functions as intended, it should detect the residual correlation between x_{4t}^* and y_{2t}^* induced by the omitted confounder. However, this relationship is not always straightforward. In some cases, the LM test may identify a correlation or directional effect between x_{4t}^* and y_{2t}^* that appears statistically significant, even when the underlying causal structure is more complex. The final selection between these specifications can be guided by overall model fit, comparing a model that includes a direct effect to one that specifies a correlation between the factors. Naturally, including the true confounder(s) in the model will improve the chi-square test statistic and overall fit indices.

Table A3. AR & CL Effects – 5-Wave RI-CLPM (Correlation)

	Estimate	Std.Err	P-value
WFX2 ~			
WFX1	0.354	0.063	0.000
WFX1	0.123	0.062	0.026
WFX2 ~			
WFX1	0.175	0.067	0.003
WFX1	0.017	0.066	0.788
WFX3 ~			
WFX2	0.253	0.054	0.000
WFX2	0.152	0.054	0.022
WFX3 ~			
WFX2	0.239	0.053	0.000
WFX2	0.249	0.052	0.000
WFX4 ~			
WFX3	0.003	0.107	0.975
WFX3	0.106	0.076	0.107
WFX4 ~			
WFX3	0.143	0.072	0.054
WFX3	0.195	0.084	0.013
WFX5 ~			
WFX4	0.225	0.056	0.001
WFX4	0.162	0.072	0.020
WFX5 ~			
WFX4	0.140	0.074	0.084
WFX4	0.273	0.050	0.000
Chi-square	155.733		
DF	169		
CFI	1.000		
NFI	0.983		
TLI	1.002		
RMSEA	0.000		

Note: All coefficients are standardized.

Figure A2. 5-Wave RI-CLPM with 2 Indicators (Direct Effect)

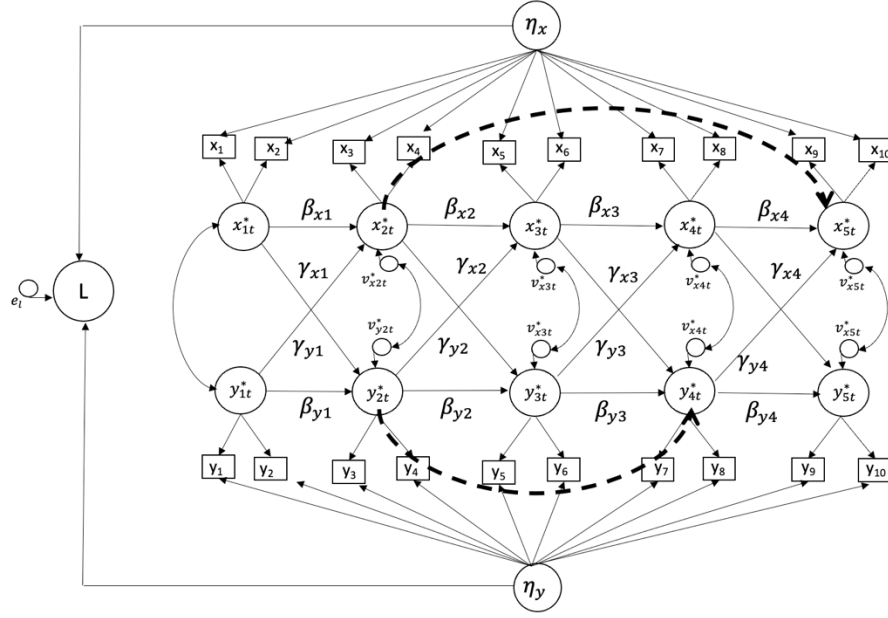


Table A4. Test Result for 5-Wave RI-CLPM with 2 Indicators (Direct Effect)

			LM χ^2	EPC	Wald Test	P-value
WFX5	~	WFX2	113.635	1.022	209.231	0.000
WFX2	~~	WFX5	95.532	0.690	2.881	0.090
WFX4	~	WFX2	94.187	-0.827	0.970	0.325
WFX2	~~	WFX4	79.406	-0.554	11.150	0.001
WFY4	~	WFY2	29.105	0.867	0.413	0.520
WFY2	~~	WFY4	25.333	0.441	0.413	0.520

Figure A2 illustrates a scenario where x_{2t}^* directly affects x_{5t}^* , and y_{2t}^* directly affects y_{4t}^* . I follow the same method that I have introduced previously to generate the population and analysis models. Table A4 shows that the 2SLW result, where both unmeasured confounders were successfully detected.

Table A5. AR & CL Effects – 5-Wave RI-CLPM (Direct Effect)

	Estimate	Std.Err	P-value
WFX2 ~			
WFX1	0.407	0.062	0.000
WFX1	0.226	0.069	0.000
WFX2 ~			
WFX1	0.155	0.069	0.037
WFX1	0.281	0.059	0.000
WFX3 ~			
WFX2	0.262	0.070	0.001
WFX2	0.264	0.080	0.000
WFX3 ~			
WFX2	0.126	0.083	0.134
WFX2	0.092	0.055	0.201
WFX4 ~			
WFX3	0.272	0.118	0.057
WFX3	-0.003	0.097	0.980
WFX4 ~			
WFX3	0.118	0.069	0.038
WFX3	0.200	0.062	0.001
WFX5 ~			
WFX4	0.131	0.077	0.011
WFX4	0.177	0.052	0.000
WFX5 ~			
WFX4	0.184	0.063	0.021
WFX4	-0.020	0.115	0.860
WFX5 ~			
WFX2	0.625	0.047	0.000
WFX4 ~			
WFX2	0.423	0.078	0.000
Chi-square	167.117		
DF	168		
CFI	1.000		
NFI	0.983		
TLI	1.000		
RMSEA	0.000		

Note: All coefficients are standardized.

Five-Wave RI-CLPM with Two Indicators Per Factor (Mediation)

Figure A3 illustrates that the 2SLW approach can identify the mediation path in the five-wave RI-CLPM with two indicators per factor. As shown, M serves as the mediator between the residuals of x_{2t}^* and x_{4t}^* (WFX4~WFX2). Table A6 shows the result of the 2SLW method, where the unmeasured mediation path was identified. Moreover, the mediation is observed regressed on x_1 , thus, the test also shows a statistically significant relationship between x_{1t}^* and x_{4t}^* (in WFX4~WFX4). To validate this

omitted parameter, I need to incorporate it into the analysis model and evaluate its statistical and substantive relevance.

Figure A3. 5-Wave RI-CLPM with 2 Indicators (Mediation)

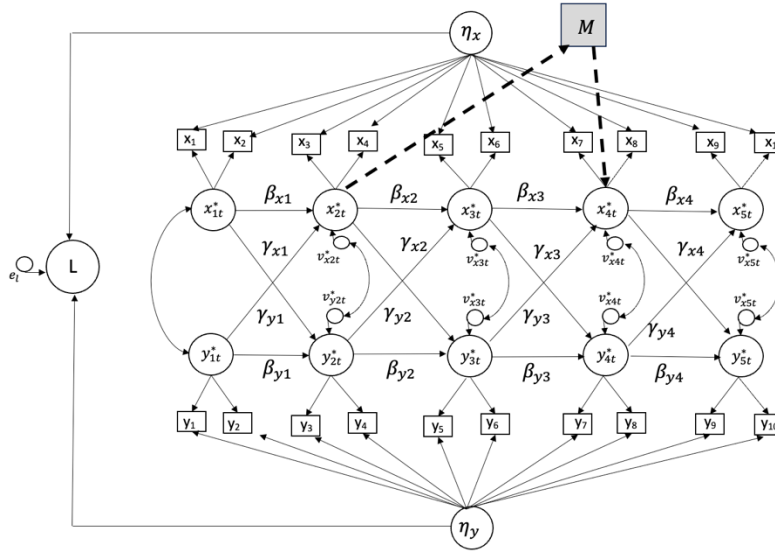


Table A6. Test Result for 5-Wave RI-CLPM with 2 Indicators (Mediation)

			LM χ^2	EPC	Wald Test	P-value
WFX4	~	WFX2	24.742	0.747	72.181	0.000
WFX2	~~	WFX5	22.761	-0.302	2.520	0.112
WFX5	~	WFX2	21.493	-0.461	0.075	0.784
WFX1	~~	WFX4	12.717	0.248	61.918	0.000
x31	~~	x32	9.273	5.633	0.017	0.898

Table A7. AR & CL Effects – 5-Wave RI-CLPM (Mediation)

	Estimate	Std. Err	P-value
WFX2 ~			
WFX1	0.085	0.081	0.275
WFX1	0.187	0.072	0.010
WFX2 ~			
WFX1	0.248	0.072	0.000
WFX1	0.065	0.072	0.325
WFX3 ~			
WFX2	0.145	0.074	0.063
WFX2	0.120	0.061	0.079
WFX3 ~			
WFX2	0.270	0.065	0.000
WFX2	0.210	0.066	0.001
WFX4 ~			
WFX3	0.042	0.073	0.369
WFX3	0.041	0.057	0.333
WFX4 ~			
WFX3	0.241	0.070	0.001
WFX3	0.086	0.075	0.216
WFX5 ~			
WFX4	0.189	0.043	0.002
WFX4	0.130	0.068	0.055
WFX5 ~			
WFX4	0.167	0.080	0.037
WFX4	0.242	0.037	0.000
WFX4 ~			
M	0.561	0.039	0.000
WFX2	0.455	0.071	0.000
M ~			
x11	0.629	0.019	0.000
Chi-square	200.318		
DF	187		
CFI	0.999		
NFI	0.981		
TLI	0.998		
RMSEA	0.008		

Note: All coefficients are standardized.

Cross-Lagged Panel Model (CLPM)

I construct a CLPM model to test the 2SLW approach, following the same simulation procedure described earlier in the paper. In the population model, AR coefficients are set to 0.5, CL coefficients to 0.2, and residual correlations within time points to 0.3. Before proceeding with the analysis, it is essential to validate the baseline CLPM population model. This baseline model serves as the foundation for generating variants to test the 2SLW approach. The baseline structure, excluding the dashed lines, is illustrated in Figure A3.

Table A8. Monte Carlo and Asymptotic Results for CLPM

N	Chi-square	SD	P-value	Rej Rate	NFI	CFI	RMSEA
100	13.060	5.332	0.444	0.076	0.981	1.000	0.000
200	12.640	5.035	0.463	0.060	0.995	1.000	0.000
300	11.923	4.850	0.501	0.046	0.994	1.000	0.000
500	12.171	5.076	0.494	0.058	0.997	1.000	0.000
800	11.746	4.906	0.521	0.064	0.995	0.998	0.027
1000	12.000	5.085	0.501	0.058	0.997	1.000	0.012
5000	11.794	4.982	0.513	0.036	1.000	1.000	0.000
10000	12.130	4.794	0.490	0.036	1.000	1.000	0.006

Note: Theoretically expected mean $\chi^2 = 12$, SD= 4.898, P -value=0.5, rejection rate=0.05.

As shown in Table A9, the chi-square test statistics are close to the degrees of freedom ($df = 12$), with a standard deviation of 4.898, an average p -value of 0.05, and an average rejection rate of 0.05. The fit indices, NFI and CFI, are near 1.0, while RMSEA approaches 0. These results indicate that the population model adheres to asymptotic properties and it is well specified.

Figure A4. Diagram of CLPM (Correlation)

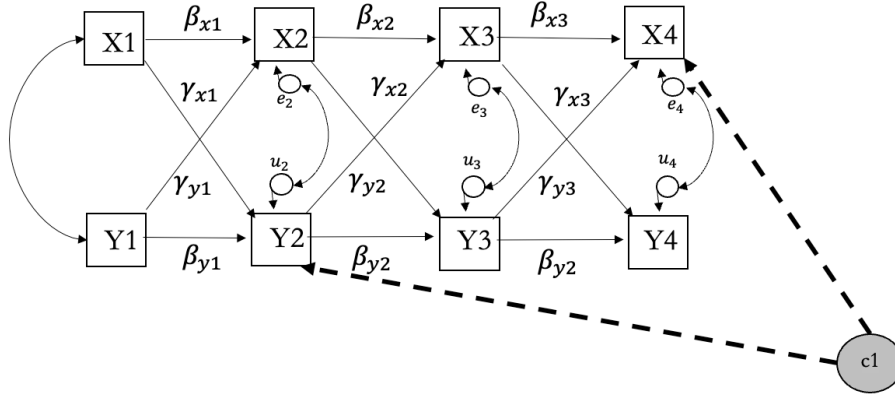


Table A9. Test Result for CLPM (Correlation)

			LM χ^2	EPC	Wald Test	P-value
X4	~~	Y2	282.919	0.426	217.073	0.000
X4	~~	Y3	210.982	-0.440	0.507	0.476
X4	~	Y2	161.480	0.411	0.282	0.595
X2	~~	X4	64.346	-0.140	0.695	0.405
Y2	~~	Y4	60.740	-0.149	0.021	0.884
Y4	~	Y2	37.786	-0.150	0.240	0.624
X2	~~	Y4	10.857	0.043	0.140	0.708
Y4	~~	Y1	3.925	0.042	3.940	0.047

Table A7 shows that the 2SLW approach successfully identified the correlation between X4 and Y2. However, it also flagged a correlation between Y4 and Y1, which was only marginally significant. After including this parameter in the model, the coefficient remained statistically insignificant, suggesting that—despite being identified by the 2SLW—it lacks substantive meaning. Therefore, I decided to exclude it from the final model.

Table A10. AR & CL Effects for CLPM (Correlation)

	Estimate	Std. Err	P-value
X2 ~X1	0.591	0.022	0.000
X3 ~X2	0.483	0.030	0.000
X4 ~X3	0.407	0.042	0.000
Y2 ~Y1	0.391	0.027	0.000
Y3 ~Y2	0.550	0.024	0.000
Y4 ~Y3	0.504	0.035	0.000
Y2 ~X1	0.191	0.027	0.000
Y3 ~X2	0.184	0.029	0.000
Y4 ~X3	0.193	0.035	0.000
X2 ~Y1	0.160	0.023	0.000
X3 ~Y2	0.250	0.025	0.000
X4 ~Y3	0.124	0.044	0.000
X4 ~Y2	0.471	0.029	0.000
Chi-square	6.826		
DF	11		
CFI	1.000		
NFI	0.998		
TLI	1.002		
RMSEA	0.000		

Note: All coefficients are standardized.

Table A8 shows that after including the confounder, the model became well specified. The autoregressive and cross-lagged coefficient estimates closely matched those of the population model. Moreover, the chi-square test statistic was 6.826 with 11 degrees of freedom, and the CFI, NFI, and TLI were all close to 1.00, with an RMSEA of zero. Together, these results confirm that the 2SLW approach successfully identified the unmeasured confounder.

Cross-Lagged Panel Model—Direct Effect

In Figure A4, I create two direct effects in the CLPM, connecting X2 and X4, as well as Y1 and Y3.

Table A8 presents the 2SLW results, which efficiently identified the unmeasured confounders: the LM test flagged potential parameters, and the Wald test confirmed the correct ones.

Figure A5. Diagram of CLPM (Direct Effect)

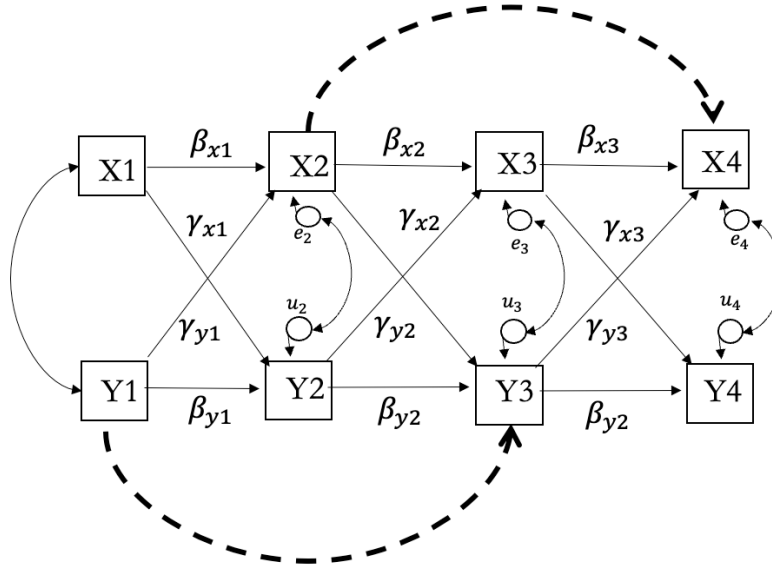


Table A11. Test Result for CLPM (Direct Effect)

			LM χ^2	EPC	Wald Test	P-value
Y3	~	Y1	477.388	0.639	914.578	0.000
Y3	~~	Y1	451.092	0.590	0.171	0.679
X4	~	X2	377.715	0.653	605.803	0.000
X2	~~	X4	174.765	0.187	0.600	0.439
X3	~	Y1	99.274	-0.239	0.418	0.518
X3	~~	Y1	96.026	-0.224	0.351	0.554
Y4	~	X2	94.751	-0.276	0.333	0.564
X4	~	X1	77.505	0.223	0.014	0.905
X4	~~	X1	77.042	0.196	0.318	0.573
Y4	~~	X1	23.087	-0.091	0.306	0.580
Y4	~	Y2	22.706	-0.157	0.534	0.465

Table A12. AR & CL Effects for CLPM (Direct Effect)

	Estimate	Std. Err	P-value
X2 ~X1	0.536	0.024	0.000
X3 ~X2	0.522	0.033	0.000
X4 ~X3	0.366	0.035	0.000
Y2 ~Y1	0.535	0.022	0.000
Y3 ~Y2	0.354	0.036	0.000
Y4 ~Y3	0.607	0.023	0.000
Y2 ~X1	0.190	0.023	0.000
Y3 ~X2	0.151	0.031	0.000
Y4 ~X3	0.159	0.032	0.000
X2 ~Y1	0.204	0.023	0.000
X3 ~Y2	0.185	0.034	0.000
X4 ~Y3	0.153	0.024	0.000
Y3 ~Y1	0.500	0.021	0.000
X4 ~X2	0.443	0.027	0.000
Chi-square	3.546		
DF	10		
CFI	1.000		
NFI	0.999		
TLI	1.003		
RMSEA	0.000		

Note: All coefficients are standardized.

Table A9 shows that, after incorporating the suggested unmeasured confounders into the original model, the chi-square test statistic and fit indices indicate excellent fit. Moreover, the AR and CL coefficients closely match those of the population model.

Cross-Lagged Panel Model—Mediation

To test whether the 2SLW approach can identify a mediation path in the CLPM, I specify the model shown in Figure A5, where M serves as the mediator between X2 and X4. The model includes both the direct effect of X2 on X4, controlling for M , and the indirect effect of X2 on X4 through M . To construct this mediation structure, I regress M on x1, inducing a high correlation between the two. Table A10 shows that the 2SLW approach identifies four unmeasured confounders. Specifically, X4

is predicted by both X2 and M , as well as by x1. Because M is regressed on x1, their LM test statistics are identical, and the Wald test reveals a multicollinearity issue between them. Therefore, we disregard the path Y4~x1 in subsequent analyses. Additionally, the 2SLW approach identifies Y4~x1 as statistically significant. To validate this suggested confounder, I include it in the revised model. As shown in Table A11, the coefficient for Y4~x1 is small and not statistically significant, indicating it carries little explanatory value. I recommend excluding this parameter from further analysis.

Figure A6. Diagram of CLPM (Mediation)

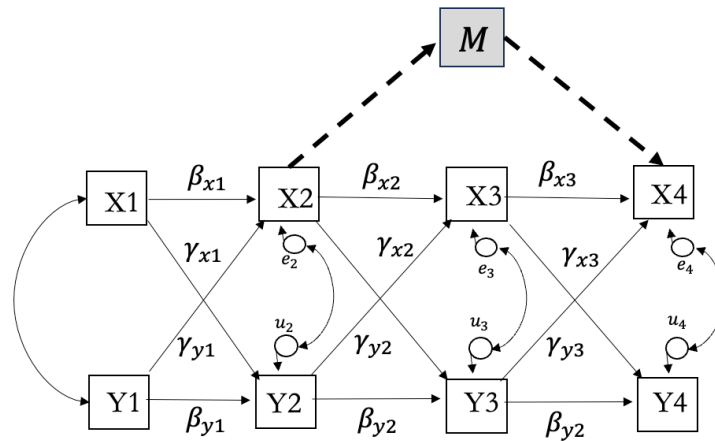


Table A13. Test Result for CLPM (Mediation)

			LM χ^2	EPC	Wald Test	P-value
X4	~	X2	304.568	0.630	438.425	0.000
X4	~	c1	172.844	0.641	451.147	0.000
X4	~	x1	172.844	0.321	5.150	0.023
X2	~~	X4	120.016	0.164	0.243	0.622
X4	~	X1	86.836	0.251	0.456	0.500
X4	~~	X1	77.244	0.222	3.075	0.079
Y4	~	X2	61.519	-0.217	0.082	0.775
Y4	~	c1	24.429	-0.185	0.139	0.709
Y4	~	x1	24.429	-0.092	5.625	0.018
Y4	~	X1	23.003	-0.099	0.606	0.436
Y4	~~	X1	22.195	-0.091	0.415	0.519
X2	~~	Y4	20.525	-0.052	0.017	0.897
c1	~	X2	13.291	-0.027	0.428	0.513
c1	~	X1	12.697	-0.024	2.432	0.119

Table A14. AR & CL Effects for CLPM (Mediation)

	Estimate	Std. Err	P-value
X2 ~X1	0.548	0.023	0.000
X3 ~X2	0.507	0.033	0.000
X4 ~ X3	0.284	0.038	0.000
Y2 ~Y1	0.521	0.023	0.000
Y3 ~Y2	0.489	0.035	0.000
Y4 ~Y3	0.528	0.035	0.000
Y2 ~X1	0.237	0.023	0.000
Y3 ~X2	0.204	0.034	0.000
Y4 ~X3	0.125	0.035	0.001
X2 ~Y1	0.194	0.023	0.000
X3 ~Y2	0.191	0.034	0.000
X4 ~Y3	0.155	0.035	0.000
c1 ~x1	0.923	0.007	0.000
X4 ~X2	0.450	0.026	0.000
c1	0.314	0.038	0.000
Y4 ~x1	0.042	0.020	0.074
Chi-square	28.972		
DF	26		
CFI	1.000		
NFI	0.996		
TLI	0.999		
RMSEA	0.011		

Note: All coefficients are standardized.

Table A11 shows that the model is well specified, as indicated by a chi-square test statistic of 28.972 with 26 degrees of freedom. All fit indices (CFI, NFI, TLI, and RMSEA) fall within acceptable ranges. Moreover, all autoregressive (AR) and cross-lagged (CL) coefficients are statistically significant, except for the path from X1 to Y4.